

Modeling turbulent mixing of an evaporating spray

G. Subramanian,* O. Colin,* A. Pires da cruz* L. Vervisch** and G. Bruneaux,*

* Institut Français du Pétrole (IFP), 1 et 4 av. Bois-Préau, 92852 Rueil-Malmaison Cedex, France

** INSA de Rouen, UMR-CNRS-6614-CORIA, France

Correspondence e-mail: ganesan.subramanian@ifp.fr

Introduction

A good understanding of the physical processes involved in turbulent reactive spray is still lacking due to its great complexity [1]. The reliability of a spray combustion model lies primarily on the base of the fuel air mixture preparation. The objective of this paper is to test scalar fluctuation closures against liquid spray evaporation LIEF visualisations. Three different closures for the evaporation source term of the mixture fraction variance equation are tested [2–4]. The contribution of each term, such as production and dissipation to the global budget of scalar fluctuation is analysed and comparisons between experimental and numerical results are made. In the first part of the paper, a brief introduction of the experimental setup and the method used for spray visualisation are presented. Following on, the three spray evaporation source term closures considered in this study are described. Finally, comparisons between experimental and model results are made based on both evaporation models and scalar dissipation algebraic closures.

Experimental study

A combustion cell built for studying spray behavior under high pressure, high temperature conditions with large optical access was used (figure 1). More details about the experimental setup and procedure can be found in references [5–7]. The gas in the cell was heated and pressurized using a pre-combustion technique in order to rise the pressure and temperature inside the cell before injection. The liquid injection takes place during the cooling phase of the burnt gases, when the desired levels of pressure and temperature are attained. This method enables studying spray evaporation without combustion coupling since the pre-combustion gas composition can be set so that pre-combustion consumes all available oxygen. The liquid fuel was injected through a high pressure, single hole nozzle (diameter 0.15 mm), common-rail, Diesel type injector. Initial test conditions were maintained as follows: Inert gas temperature and pressure at the time of injection were respectively 800K and 60×10^5 Pa. Injection pressure was kept at 1500×10^5 Pa. The fuel mixture was composed of 70% n-decane and 30% α -methyl-naphthalene. Instantaneous images of fuel vapor distribution were obtained using the Laser Induced Exciplex Fluorescence (LIEF) technique. They were then post-processed using statistical methods in order to extract average values and fluctuations of vapor fuel mass concentration.

Spray visualisation by LIEF imaging technique

The Laser Induced Exciplex Fluorescence (LIEF) technique illustrated in figure 2 has been applied for quantitative imaging of the gas phase fuel mass density. A brief description of the measurement technique and image post processing is given here. A tripled YAG laser of wavelength 355nm was used to illuminate the vapor part of the spray. A cylindrical lens coupled with a spherical lens was used to obtain a laser sheet of 1mm width at the nozzle hole location. A fluorescent tracer initially mixed with the fuel mixture helps to illuminate the vapor phase of the fuel. The scattered fluorescent light is recorded by a high-resolution CCD Digital pixel camera. A photodiode is placed in parallel to collect the intensity I_0 of each laser pulse. This was used to estimate the uncertainty of the measurements. More details can be found in [6, 7]. The mass concentration of the vapor fuel at a given location is determined from the image collected by the

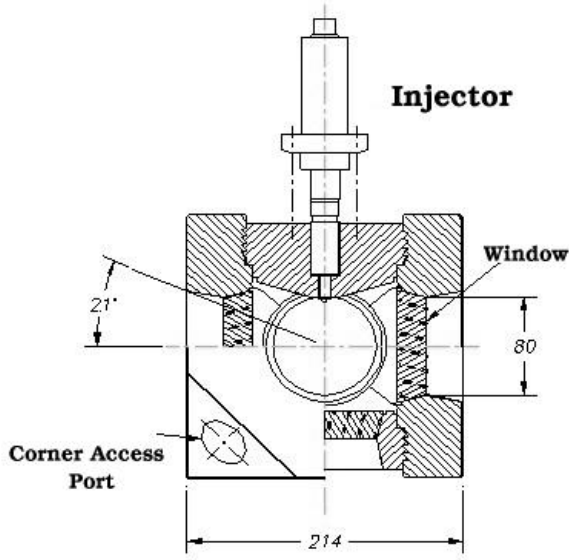


Figure 1: *Experimental setup*

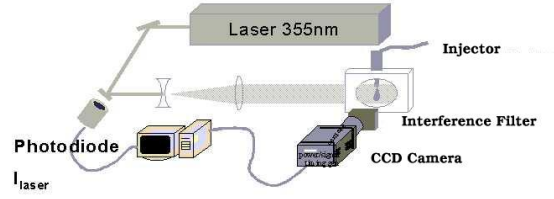


Figure 2: *Principle of LIEF imaging*

CCD camera using the following expression:

$$\rho_{Fu}(x, y) = \frac{I(x, y)}{KI_0(y)} = \frac{I(x, y)}{I_0(y)} \times \frac{M}{I_v} \quad (1)$$

where $\rho_{Fu}(x, y)$ is the mass concentration of fuel at location (x, y) , $I(x, y)$ is the intensity of the fluorescence collected, K is a proportionality factor, $I_0(x, y)$ is the laser intensity measured by the photodiode, M is the total mass of the fuel injected measured during calibration and I_v is the volume intensity of the image calculated by integrating the normalised intensity of the fluorescence. Uncertainty analysis including all measurements shows that a 80% level of confidence can be anticipated.

Statistical analysis for Fluctuations

Instantaneous images were post treated using statistical methods in order to extract average values and fluctuations of fuel mass density. For this purpose, a number of images varying from 5 to 50 were recorded for each time step during the experiment. For a given time step, average values were obtained using the following relation:

$$\bar{\rho}_{Fu}(x, y) = \sum_{i=1}^{i=n} \rho_{Fu}(x, y) / n \quad (2)$$

where n is the number of images recorded at a given time. Fluctuations of fuel mass density can be obtained using the relation as follows:

$$\Psi(x, y) = \sum_{i=1}^{i=n} (\rho_{Fu}(x, y) - \bar{\rho}_{Fu}(x, y))^2 / n \quad (3)$$

It has to be noted here that the experimental values of the local total mass density ($\rho_{ch}(x, y)$) are not available due to the major difficulty in measuring the local temperature of the gases.

Modeling study

The aim of this paper is to better understand the behavior of mixture fraction variance when liquid spray evaporation is present. For this purpose, each source term of the balance equation

of the Favre averaged mixture fraction variance $\tilde{v} = \widetilde{Z''^2}$ is evaluated. In this work, we focus on testing the spray evaporation closure term for variance against experimental results.

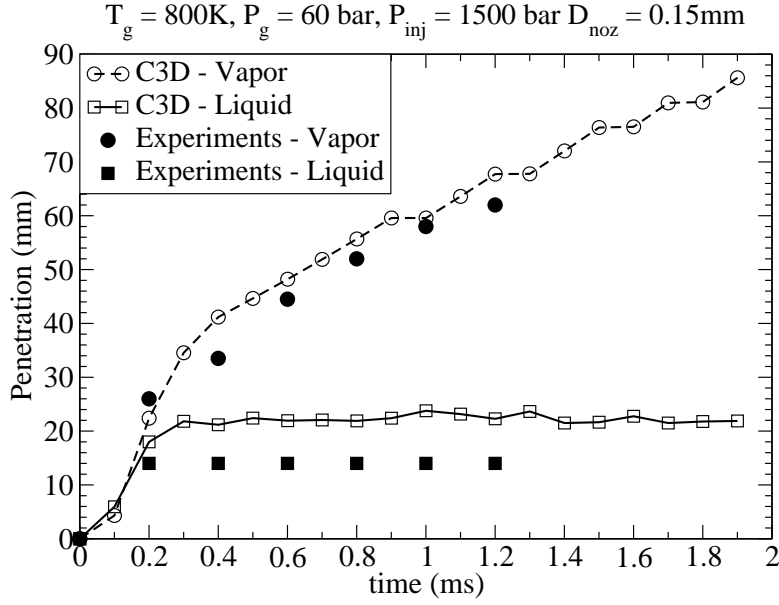


Figure 3: Spray penetration data

Liquid fuel injection and evaporation have been simulated using the spray atomization and break-up WAVE-FIPA [5] model implemented in the IFP-C3D engine code [8] which parameters were adjusted to match the experimental results of liquid and vapor fuel penetration. Figure 3 shows the comparison between the model and experimental results for the two phases. The constant in the expression for the break-up time in the WAVE-FIPA break-up model [5] is set to 20 and the Sauter Mean Radius (SMR) is set to 0.075 mm.

A brief description of the scalar fluctuation model implemented in the IFP-C3D RANS solver [8] is presented here. The transport equation for the Favre averaged variance \tilde{v} is:

$$\frac{\partial \tilde{v}}{\partial t} + \frac{\partial \tilde{v} u_i}{\partial x_i} = \frac{\partial}{\partial x_i} \left(\frac{\mu}{S_c} \frac{\partial \tilde{v}}{\partial x_i} \right) - \underbrace{\frac{\partial \tilde{v} u_i}{\partial x_i}}_{(I)} - \underbrace{2 \tilde{v} u_i Z'' \frac{\partial Z}{\partial x_i}}_{(II)} - \underbrace{2 \frac{\mu}{S_c} \left(\frac{\partial Z''}{\partial x_i} \right)^2}_{(III)} + \underbrace{\tilde{v} \dot{S}_v}_{(IV)} \quad (4)$$

where μ is the fluid viscosity and S_c is the Schmidt number. Appropriate models for the unclosed terms *I*, *II*, *III*, *IV* are necessary. Turbulent transport (*I*) and production terms (*II*) are modeled with the classical gradient transport assumption. The Scalar dissipation rate χ term (*III*) is closed algebraically following a linear relaxation hypothesis [9]:

$$\chi = 2\mu/\bar{\rho}S_c(\partial Z''/\partial x_i)^2 = C(\epsilon/\kappa)\tilde{v} \quad (5)$$

where κ is the turbulent kinetic energy, ϵ is its dissipation and C is a constant. Spray evaporation term for variance (*IV*) is defined as [4]:

$$\dot{S}_v = 2Z''\dot{S} - 2\tilde{Z}Z''\dot{S} - Z''^2\dot{S} \quad (6)$$

where \dot{S} is the fuel mass evaporation source term. Following [4], the \dot{S}_v term can be reorganized as:

$$\dot{S}_v = \tilde{S}_v^+ + \tilde{S}_v^- \quad (7)$$

where $\tilde{S}_v^+ = 2Z''\dot{S}(1 - \tilde{Z})$ and $\tilde{S}_v^- = -Z''^2\dot{S}$.

As different closures for this term can be found in the literature, three models were chosen for this study. The models proposed by Demoulin and Borghi [2], here onwards indicated as *DB*, Hollmann and Gutheil [3] indicated as *HG*, and the single droplet model (SDM) proposed by Réveillon and Vervisch [4] cited as *RV* were considered. These models are briefly discussed in

the following sections. Individual contribution of terms *II* and *III* found in equation 4 are then evaluated separately in order to understand the influence of each of them in the production and destruction of variance relative to the evaporation source term *IV*.

Model by Demoulin and Borghi (*DB*)

The main assumption behind this model is that the vapor fuel source term \dot{S} is only relevant around the droplet surface. Hence, the local mixture fraction Z is close to the saturation value Z^* observed at the droplet surface. Therefore, $\widetilde{Z\dot{S}}$ term can be approximated by $Z^*\widetilde{\dot{S}}$. After algebraic manipulations, $\widetilde{Z''\dot{S}} = \widetilde{\dot{S}}(Z^* - \widetilde{Z})$. The $\widetilde{\dot{S}_v^-}$ term is approximated by $\widetilde{Z''^2\dot{S}}$. The final *DB* source term may then be written as :

$$\widetilde{\dot{S}_v^-}^{DB} = \widetilde{\dot{S}}(Z^* - \widetilde{Z})(2 - Z^* - \widetilde{Z}) \quad (8)$$

Model by Hollmann and Gutheil (*HG*)

If we suppose that Z and \dot{S} are correlated, which is a reasonable assumption on an evaporation problem, the following relations can be derived: $\widetilde{Z} = \alpha\widetilde{\dot{S}}$ and $Z'' = \alpha\dot{S}'' \Rightarrow \widetilde{Z''\dot{S}''} = \widetilde{Z''^2\dot{S}}/\widetilde{Z}$. According to [3], if such correlation is only partial, then $\widetilde{Z''\dot{S}''}$ can be split into a correlated part $C\widetilde{Z''\dot{S}''}$ and a non correlated part $(1 - C)\widetilde{Z''\dot{S}''}$ with C being a correlation factor. Then,

$$\widetilde{Z\dot{S}} = C\widetilde{Z^2\dot{S}}/\widetilde{Z} + (1 - C)\widetilde{Z\dot{S}} \quad (9)$$

The $\widetilde{\dot{S}_v^-}$ term is modeled as in *DB*. Using previous relations with C=1/2 as proposed in [3] the final expression for the evaporation source term $\widetilde{\dot{S}_v^-}^{HG}$ is obtained:

$$\widetilde{\dot{S}_v^-}^{HG} = \widetilde{Z''^2\dot{S}}(1 - 2\widetilde{Z})/\widetilde{Z} \quad (10)$$

SDM by Réveillon and Vervisch (*RV*)

Based on DNS calculations of evaporating droplets of a dilute spray in a turbulent flow field, the authors [4] have shown that the conditional source term $(\dot{S} | Z)$ can be approximated as a monotonic function of Z :

$$(\dot{S} | Z) = \alpha_{B_Y} Z^\xi \quad (11)$$

where α_{B_Y} is a function which depends on the local spray properties. The exponent ξ is determined dynamically by the authors [4] using a constraint that the PDF integral of function 11 over Z must yield the correct Eulerian source term as given by the CFD code.

$$\widetilde{\dot{S}} = \int_Z \alpha_{B_Y} Z^{+\xi} P(Z^+) dZ^+ \quad (12)$$

where $P(Z^+)$ is the probability density function of the mixture fraction which is presumed to follow a β distribution. More details can be found in [4]. However, in this study ξ is set to 2 as proposed in [4]. Therefore the final mean evaporation source terms are expressed as:

$$\widetilde{\dot{S}_v^-}^{+RV} = 2(1 - \widetilde{Z}) \int_0^{\widetilde{Z}^s} (Z^+ - \widetilde{Z}) (\dot{S} | Z) P(Z^+) dZ^+ \quad (13)$$

$$\widetilde{\dot{S}_v^-}^{-RV} = - \int_0^{\widetilde{Z}^s} (Z^+ - \widetilde{Z})^2 (\dot{S} | Z) P(Z^+) dZ^+ \quad (14)$$

This closure has also been implemented in the IFP-C3D code using a tabulation strategy. A lookup table has been built a priori as a function of certain mean mixture fraction (\tilde{Z}) and segregation factor values which is defined as:

$$S = \frac{\tilde{Z}^{1/2}}{\tilde{Z}(1 - \tilde{Z})} \quad (15)$$

Depending on the local mixture conditions and fluctuations inside the cell, evaporation sources are linearly interpolated inside the lookup table.

Results and Discussion

In the first part of this section, results corresponding to average fuel mass density obtained by the experiments and the numerical simulations are presented. In the second part, the results corresponding to the fuel mass fluctuations are discussed in detail. Simulations were conducted using three different values (1,2 and 4) for constant C in the scalar dissipation rate model (term III in equation 4). It was found that in comparison with LIEF images, the value $C = 2$, which is commonly used in the literature [9], gives the best results and hence was retained in this study. Experimental results are available at time instants 0.2, 0.4, 0.6, 0.8, 1.0, 1.2 and 1.4ms.

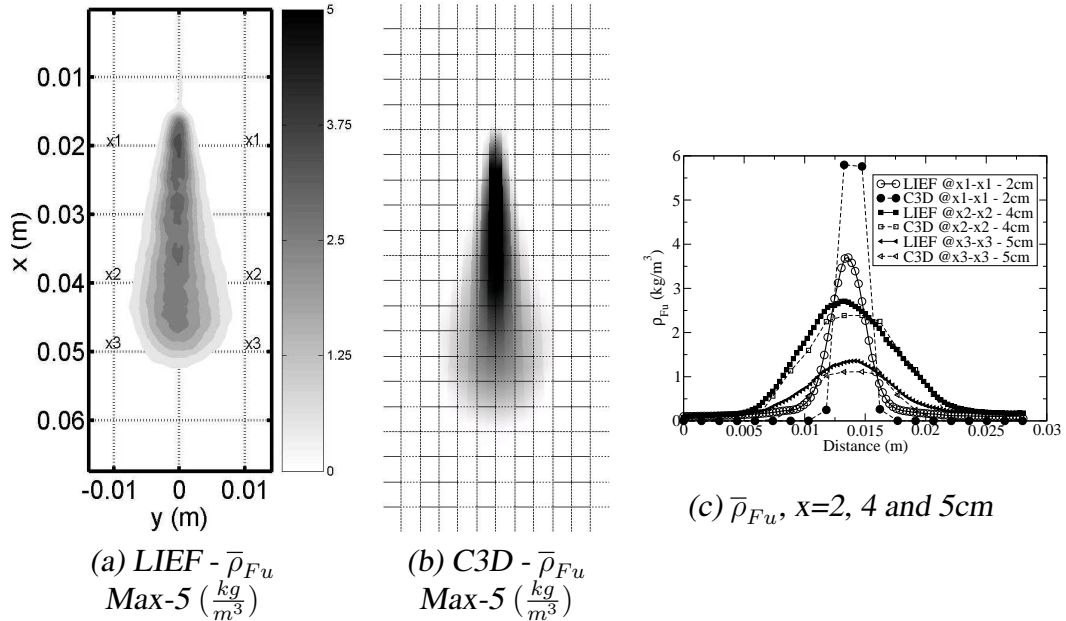


Figure 4: Average fuel concentrations at $t=0.8ms$ - Experiments and simulations.

Figure 4 shows the comparison between the experiments and the simulations of average fuel mass density at time $t = 0.8ms$. Figures 4(a) and 4(b) represent respectively the average fuel density field obtained by LIEF measurements and the IFP - C3D RANS code. The gray scale for the above two figures is the same and its maximum value is $5.0kg/m^3$. Figure 4(c) shows the fuel density profiles at various cross-sections along the injector axis x . Close to the injector, at cross section x1-x1 (20 mm away from the injector), calculations over-predict fuel density profiles. This can be attributed to well known difficulties inherent to lagrangian spray models. Further downstream, at cross-sections x2-x2 and x3-x3 (respectively 40 mm and 50 mm away from the injector), fuel concentration profiles obtained from experiments and calculations show good agreement.

Figure 5 shows the comparison of fuel mass fluctuations between LIEF experiments (5(a)), model DB [2] (5(b)), model HG [3] (5(c)) and model RV [4] (5(d)). All units are $(kg/m^3)^2$. The maximum value of the gray scale in each figure is indicated accordingly. It can be seen from figures 5(b), 5(c) and 5(d) that qualitatively, all models DB , HG and RV correctly reproduce the experimental scalar fuel fluctuation field. However, quantitatively, model DB predicts higher levels of fluctuations than models HG , and RV . In the experiments, fuel mass fluctuations vary

from 0 to a maximum of $1.5 (kg/m^3)^2$ whereas in calculations with model *DB*, the maximum value lies around $9.0(kg/m^3)^2$ and with model *HG* it is $3.0(kg/m^3)^2$. Maximum fluctuation level calculated with model *RV* is around $8.0(kg/m^3)^2$.

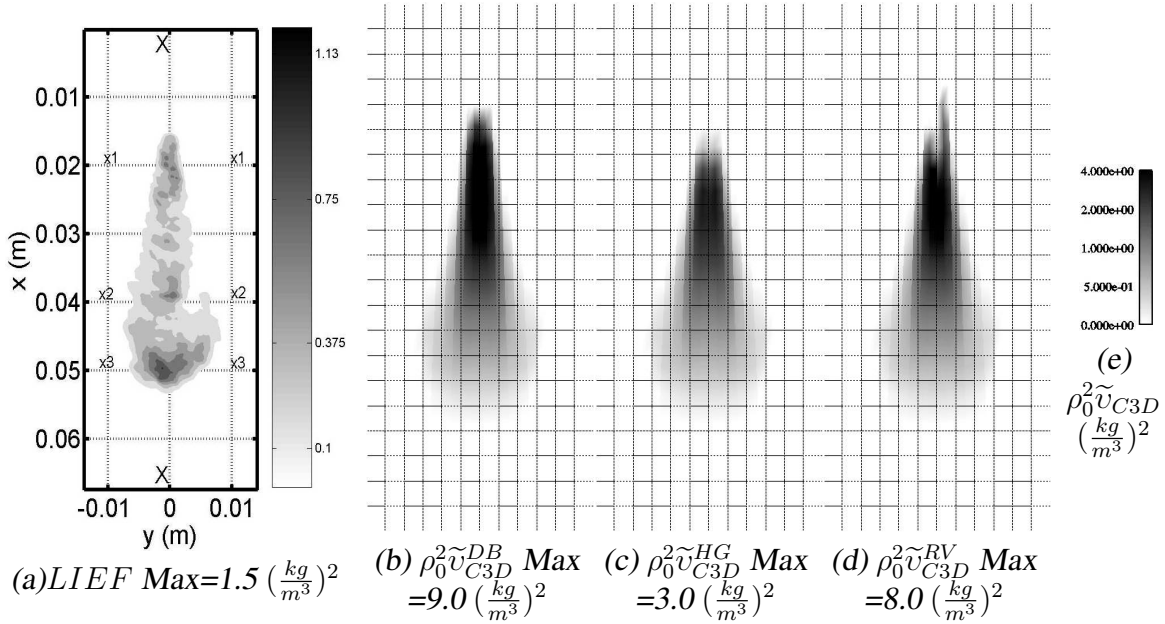


Figure 5: Fuel mass fluctuations at $t=0.8ms$ - LIEF, models *DB*, *HG* and *RV*.

The importance of the \tilde{S}_v term relative to production and dissipation terms was also studied. Figures 6(a), 6(b) and 6(c) show respectively the spray evaporation source term fields using model *DB*, model *HG* and model *RV* in units (1/s). It was observed that terms *II*, *III* and *IV* in equation 4 have the same order of magnitude. This means that in liquid spray evaporation configuration, scalar fluctuations induced by spray evaporation cannot be neglected. This is particularly important in the liquid-vapor interface zone where according to figures 6(a) - 6(c), this term has a non negligible contribution to the global fluctuation level.

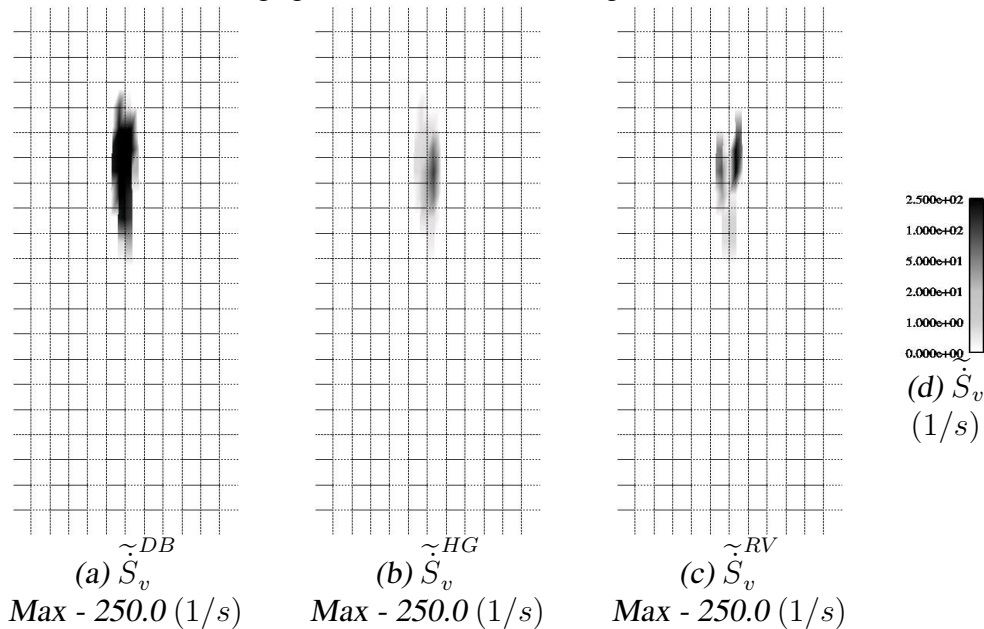
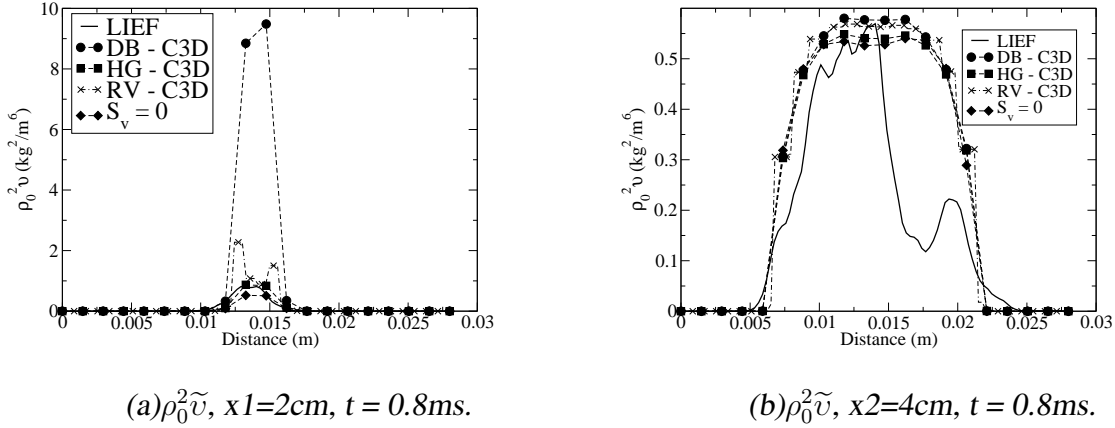


Figure 6: Spray evaporation source \tilde{S}_v at $t=0.8ms$ - models *DB*, *HG* and *RV*.

Figures 7(a) and 7(b) present fluctuation cross-section profiles and figure 8 presents fluctuations along the x axis as indicated in figure 5(a). Up to 35 mm away from the injector (figure 8), fluctuation levels are overestimated by all models by a maximum factor of 10 for model *DB*, 3 for model *HG* and around 8 for model *RV* when compared to LIEF results (see cross section $x1-x1$ in figure 7(a)). Profiles obtained without spray evaporation closure ($\tilde{S}_v = 0$) are also shown

in these figures. These profiles are close to those obtained with model *HG* indicating that model *HG* source term is globally small when compared to the balance between source terms (II) and (III). However, as it has been mentioned before, the relative importance of the three source terms is similar in the evaporation zone (around $x=20\text{mm}$). Since even for case ($S_v = 0$), the fluctuation level is overestimated close to the injector, we can conclude that this is mainly due to the over-prediction of the mean fuel concentration in this zone as shown in figure 4(c) at cross section $x1-x1$. We can therefore assume that given the influence of the fluctuation spray evaporation term confirmed by large differences between models *DB*, *RV* and *HG*, a correct prediction of the average fuel mass fraction close to the injector would enhance the relative importance of this source term.



(a) $\rho_0^2 \tilde{v}$, $x1=2\text{cm}$, $t = 0.8\text{ms}$.

(b) $\rho_0^2 \tilde{v}$, $x2=4\text{cm}$, $t = 0.8\text{ms}$.

Figure 7: Fuel mass fluctuation profiles - cross-sections $x1$ (a) and $x2$ (b).

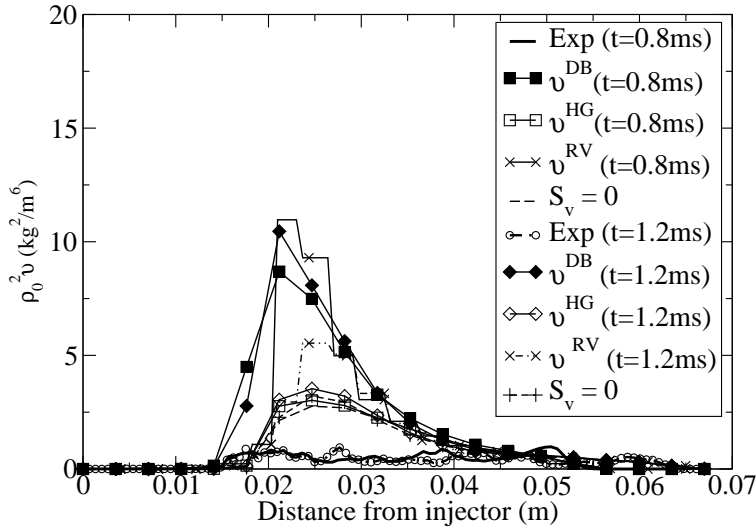


Figure 8: Fuel mass fluctuation profiles along injector axis X . $\rho_0^2 \tilde{v}$, $t = 0.8, 1.2\text{ms}$.

Finally, the discrepancy between models *DB* and *HG* can be explained by the fact that model *DB* represents the maximum possible variance source term where the evaporated fuel is considered to be introduced at saturation conditions Z^* , which means that: $\widetilde{Z'' \dot{S}}^{DB} = (Z^* - \widetilde{Z}) \widetilde{\dot{S}}$. On the contrary, in model *HG*, this correlation is modeled as: $\widetilde{Z'' \dot{S}}^{HG} = C \widetilde{Z''^2 \dot{S}} / \widetilde{Z}$. As $\widetilde{Z''^2} \leq \widetilde{Z}(Z^* - \widetilde{Z})$, we conclude that $\widetilde{Z'' \dot{S}}^{HG} \leq C \widetilde{Z'' \dot{S}}^{DB}$. Model *RV* should be more accurate as it considers the joint statistics of mixture fraction Z and evaporation source $\widetilde{\dot{S}}_v$. However, it was established and validated for dilute spray cases like gasoline injection applications.

In the downstream part of the gaseous jet ($x > 40\text{mm}$), models *DB*, *HG* and *RV* (and $S_v = 0$) give similar results in agreement with experiments as shown in figures 7(b) and 8. This indicates that the influence of the evaporation source term (IV) in the variance equation is limited to the liquid/vapor interface region. Downstream, fluctuations are essentially controlled by the balance between terms (II) and (III). This is interesting from a modeling point of view as it means that the error in modeling the spray source term (IV) in the configuration presented here has limited influence in space and time.

Conclusions and Perspectives

This paper has addressed the issues of scalar variance and dissipation model testing and validation against experimental observations. The experiments concern high pressure liquid fuel injection and spray evaporation in an atmosphere close to Diesel engine conditions. The results described here have shown that :

- The evaporation source term in the mixture fraction variance equation cannot be neglected. Inside the core of the spray, its order of magnitude is close to the variance production and dissipation terms due respectively to average mixture fraction gradient and scalar dissipation rate.
- Three models for the evaporation source term in the variance equation have been tested. In the experimental conditions used here, the Hollmann and Gutheil model performed better than the models by Demoulin and Borghi and Réveillon and Vervisch which both over-predict variance due to evaporation.
- This evaporation source term influences the fluctuation level in a limited zone close to the liquid spray (up to 40 mm away from the injector in our case). Further downstream, fluctuations are controlled by production/destruction from mean gradients and scalar dissipation.
- The classical algebraic model has been used to close the scalar dissipation rate term. Results have shown good agreement with experiments when the modeling constant was set to 2, the commonly used value in the literature.

Future work involves :

- The implementation and testing of a scalar dissipation rate modeled transport equation as proposed by Colin and Benkenida [1].
- Extension of the variance and scalar dissipation rate model equations validation to other types of experimental setup. This includes high pressure gas spray injection (without evaporation) as well as gasoline engine type direct injection where the liquid spray is dispersed.

Acknowledgements

Authors would like to thank D. Verhoeven for his assistance to treat experimental LIEF images and K. Truffin for fruitful suggestions.

References

- [1] O. Colin et A. Benkenida (2003). A new scalar fluctuation model to predict mixing in evaporating two-phase flows. *Combustion and Flame*, **134**:207-227.
- [2] F. X. Demoulin et R. Borghi (2002). Modeling of Turbulent Spray Combustion with Application to Diesel Like Experiment. *Combustion and Flame*, **129**:281-293.
- [3] H. Hollmann et E. Gutheil (1996). Modeling of Turbulent Spray Diffusion Flames Including Detailed Chemistry. *Proceedings of the Twenty-Sixth International Symposium on Combustion*.
- [4] J. Réveillon et L. Vervisch (2000). Spray Vaporization in Nonpremixed Turbulent Combustion Modeling: A Single Droplet Model. *Combustion and Flame*, **121**:75-90.

- [5] C. Habchi, D. Verhoeven, C. H. Huu, L. Lambert, J. L. Vanhemetryck et T. Baritaud (1997). Modeling Atomization and Break up in High - Pressure Diesel Sprays. Society of Automotive Engineers, (970881).
- [6] G. Bruneaux (2001). Liquid and Vapor Spray Structure in High Pressure Common Rail Diesel Injection. Atomization and Sprays, **11-5**:533-556.
- [7] G. Bruneaux (2005). Study of the Mixing Process in High Pressure Diesel Jets by Normalized Laser Induced Exciplex Fluorescence - Part I: The Free Jet Configuration. SAE Fuel & Lubricants Exposition and Meeting,
- [8] M.Zolver, D.Klahr, J.Bohbot, O.Laget et A.Torres (2003). Reactive CFD in Engines with a New Unstructured Parallel Solver. Oil and Gas Science and Technology - Review IFP,.
- [9] N. Peters (1984). Laminar Diffusion Flamelet Models in Non-Premixed Turbulent Combustion. Prog. Energy Combust. Sci., **10**:319-339.